World Cancer Research Journal

WCRJ 2026; 13 : e2994
DOI: 10.32113/wcrj_20262_2994

EXPRESSION AND PROGNOSTIC VALUE OF M6 METHYLATION REGULATORY FACTOR IN COLORECTAL CANCER

W.-Q. WANG[1,2], Z.-H. WANG[1,2], Y.-P. ZHANG[1], Y.-F. GAO[1], T.-X. MA[1,3], Y.-J. HUANG[1,2]

• • •

[1]Beijing Engineering Research Center of Food Environment and Public Health, Minzu University of China, Beijing, China
[2]School of Information Engineering, Minzu University of China, Beijing, China
[3]Key Laboratory of Ecology and Environment in Minority Areas (National Ethnic Affairs Commission), College of Life and Environmental Sciences, Minzu University of China, Beijing, China

Wenqi Wang and Zhaohua Wang contributed equally to this work

Corresponding Author
Tianxiao Ma, Ph.D; email: matianxiao@muc.edu.cn

ABSTRACT – *Objective:* N6-methyladenosine (m6A) methylation regulators are critical for cancer progression, but published data on the mechanism of m6A modification in tumor microenvironment (TME) cell infiltration of colorectal cancer (CRC) remains limited. This study aimed to investigate the correlation between m6A modification patterns and CRC TME heterogeneity and explore their prognostic significance and guiding value for immunotherapy.

Materials and Methods: RNA expression profiles and clinical data of CRC were retrieved from The Cancer Genome Atlas (TCGA) and Gene Expression Omnibus (GEO). Unsupervised clustering was performed to evaluate m6A modification patterns of 23 m6A methylation regulators in 983 CRC samples, and their associations with TME cell infiltration characteristics were systematically analyzed. Gene Ontology (GO) and gene set variation analysis (GSVA) explored underlying mechanisms, while principal component analysis (PCA) constructed an m6A score to quantify modification patterns.

Results: m6A methylation regulators showed high genetic and expression heterogeneity in CRC, leading to three distinct modification patterns. These patterns closely matched three immunophenotypes (immune rejection, immune inflammation, and immune desert) and exhibited distinct biological functions. Univariate and multivariate Cox regression indicated m6A score as an independent prognostic factor (HR=1.010, 95% CI: 1.002-1.019; HR=1.009, 95% CI: 1.000-1.017). Low m6A scores correlated with higher tumor mutation load, PD-L1/CTLA-4 expression, and poor survival. In the CTLA-4 immunotherapy cohort, high m6A scores were associated with significantly better immune response and clinical benefit (p=3.4e-06).

Conclusions: m6A methylation modification patterns are key drivers of TME heterogeneity and complexity in CRC. Exploring the relationship between m6A modification patterns and TME aids in formulating CRC immunotherapy strategies and provides valuable prognostic guidance.

KEYWORDS: m6A, Colorectal cancer, Mutation burden, Tumor microenvironment, Immunotherapy.

INTRODUCTION

Colorectal cancer (CRC) is a global health concern, ranking as the third most common cancer worldwide and the fourth leading cause of cancer-related death[1]. Although the incidence and mortality rates have declined in recent years, there has been an increase in the occurrence of this disease among younger and middle-aged populations[2]. CRC is often found at advanced stages due to its association with hereditary cancer and inflammatory bowel disease, posing challenges for effective treatment[3]. Therefore, developing precise and effective strategies for the early diagnosis and treatment of CRC is critical to reduce the incidence and improve survival rates.

N6-methyladenosine (m6A) is the most prevalent internal modification of messenger RNA (mRNA) and long non-coding RNA (lncRNA) in eukaryotes, first discovered in 1970[4]. M6A methylation regulators are known to play a significant role in cancer development, particularly in cell proliferation, migration, and invasion[5]. The m6A methylation process, dynamically regulated by RNA methylation regulators ("writers", "erasers" and "readers"), is linked to the occurrence and progression of cancer[6]. For example, the effects of m6A modification and the deregulation of m6A methylation regulators have been described in melanoma (MEL)[7]. In liver cancer, an imbalance of YTH domain family (YTHDF) reader proteins has also been shown to promote the development of viral hepatitis[8].

Although numerous studies have established a close relationship between m6A regulators and cancer, most of these investigations have focused on the role of individual regulators, resulting in context-dependent and sometimes even contradictory findings. For example, increased expression of methyltransferase-like 3 (METTL3) has been noted in patients with acute myelogenous leukemia (AML), promoting carcinogenesis[9]; In glioblastoma (GBM), a decrease in METTL3 or METTL14 expression promotes the growth of glioblastoma stem-like cells (GSC), thereby increasing tumor development[4]. In non-small cell lung cancer (NSCLC), METTL3 plays a driving role in cancer cell growth, survival, and invasion[10]. In CRC, scholars have shown that METTL3 promotes the development of CRC *in vitro* and *in vivo*[11]. However, the overall role of the entire m6A regulatory network remains poorly understood. The single-gene research approach provides incomplete information and limits the development of m6A-based clinical biomarkers.

The pathogenesis of tumors is complex, involving the cooperation of genetic factors and the tumor microenvironment (TME), in which the m6A modification also plays a critical role. Lymphocytes in the TME and their associated factors can regulate tumor occurrence, development, and invasion[12]. Myeloid-Derived Suppressor Cells (MDSCs) comprise up to 40% of the immune infiltrate in gliomas and secrete immunosuppressive factors that reduce the efficacy of immunotherapy by inhibiting T-cells[13]. Additionally, decreased expression of colony-stimulating factor 1 receptor (CSF1R), which is regulated by DNA methylation, promotes growth, invasion, and migration of hepatocellular carcinoma (HCC) by tumor-associated macrophages (TAMs)[14]. Previous studies[15,16] have mainly examined the relationship between a specific m6A methylation regulator and a particular immune cell type, but have not systematically characterized how global m6A modification patterns shape the immune landscape of the TME. To gain deeper insights into the interaction between m6A mechanisms and the anti-tumor immune response, a more comprehensive research approach is required. This study aims to elucidate the role of m6A methylation in combination with the CRC TME, thereby exploring potential targets for tumor therapy.

To achieve this aim, we downloaded the CRC dataset and clinical data from the Gene Expression Omnibus (GEO) (https://www.ncbi.nlm.nih.gov/geo/) and The Cancer Genome Atlas (TCGA) (http://cancergenome.nih.gov/) databases. We analyzed a series of m6A methylation regulators and their related genes, annotated their functions and pathways, and developed and validated a novel quantitative m6A scoring signature. As the key clinical implication of this study, this scoring system integrates the complex biological information of m6A-related genes into a single, clinically applicable, patient-specific indicator. Using this score, we systematically evaluated the tumor microenvironment (TME), predicted patient prognosis, and explored its potential as a biomarker to guide immunotherapy, thereby providing new insights into the personalized treatment of CRC patients.

MATERIALS AND METHODS

Data Downloading and Preprocessing

This study investigated CRC using data from TCGA (http://cancergenome.nih.gov/) and GEO (https://www.ncbi.nlm.nih.gov/geo/). A total of 398 CRC samples and 39 normal samples were screened for gene expression data, mutations, and clinical data. The GEO dataset GSE39582, containing gene expression data for 585 CRC samples and their clinical data, was obtained and analyzed. Table 1 provides detailed information on the GSE39582 dataset, including survival time, survival status, age, gender, stage, grade, and TNM stage. The copy number of CRC was obtained from the University of California, Santa Cruz Xena data hub (UCSC Xena). Perl software and R software's "limma[17]" package were used to merge and annotate the TCGA gene expression data and GSE39582, and FPKM format from TCGA was converted to transcripts per kilobase million (TPM) format. Copy number variation (CNV) analysis was performed and visualized using the R software's "RCircos" package, and somatic mutation was detected using the "maftools" package. Table 1 provides additional details on the GEO dataset GSE39582 used in this study.

Table 1. Information of the GEO dataset.

Dataset	Reference	Plantform	Tumor	Normal
GSE39582	[16]	[HG-U133_Plus_2] Affymetrix Human Genome U133 Plus 2.0 Array	585	0

Consensus Molecular Clustering of m6A Methylation Regulators

In this study, we investigated the role of m6A methylation regulatory factors in CRC. A comprehensive list of 23 m6A methylation regulators, including 8 writers (METTL3, METTL14, METTL16, WTAP, VIRMA, ZC3H13, RBM15, RBM15B), 13 readers (YTHDC1, YTHDC2, YTHDF1, YTHDF2, YTHDF3, HNRNPC, FMR1, LRPPRC, HNRNPA2B1, IGFBP1, IGFBP2, IGFBP3, RBMX), and 2 erasers (FTO, ALKBH5), was compiled from published literature. We detected different m6A methylation modifications in CRC based on the expression of the 23 m6A methylation regulators.

To identify the relationship between m6A methylation regulators' expression and survival, we used univariate Cox model[19] analysis with *p*-value less than 0.05 as a threshold for significance. To further classify CRC samples based on m6A methylation modifications, we performed unsupervised cluster analysis using the "ConsensusClusterPlus[20]" package in R software. The *k*-values were calculated and increased from 2 to 9. We selected the stable *k*-value based on the cumulative function distribution curve and the number of samples in each subtype, which allowed us to identify different m6A methylation modifications in CRC. Overall, our findings provide important insights into the role of m6A methylation regulatory factors in CRC and may have implications for developing targeted therapies.

Gene Set Variation Analysis (GSVA) and Gene Ontology (GO), Kyoto Encyclopedia of Genes and Genomes (KEGG) Pathway Enrichment Analysis

In order to investigate the differences in functions and pathways among different gene clusters, we utilized the Gene Set Enrichment Analysis (GSEA) (www.gsea-msigdb.org/gsea/index.jsp) database and downloaded the gene set pathway file. To conduct our analysis, we utilized R software packages such as "limma[17]", "GSEABase[21]", and "GSVA[22]". An important part of our analysis involved using the "GSVA" package to perform kernel estimation of the cumulative density function (TCDF) on our gene expression matrix. This allowed us to sort the genes by expression levels, calculate Kolmogorov-Smirnov-like rank statistics for each gene set, and output a matrix containing the enrichment fractions of gene sets and sample pathways[22].

Furthermore, we used the "org.Hs.eg.db", "DOSE[24]", "clusterProfiler[23]", and "enrichplot[25]" packages of R to perform enrichment analysis of GO pathways (*p*-value = 0.05, adj. *p* = 0.05) and KEGG pathways (*p*-value = 0.05, adj. *p* = 1) functions. Overall, our analysis allowed us to gain important insights into the functional and pathway differences among different gene clusters and provided valuable information for understanding the underlying mechanisms of CRC.

Differential Analysis of Immune Cells by Single-Sample Gene Set Enrichment Analysis (ssGSEA)

We utilized the immune cell gene set curated by Pornpimol Charoentong[26] to analyze the TME infiltration of m6A subtype. To perform this analysis, we employed R software packages including "GSVA[22]", "GSEABase[21]", and "limma[17]".

To calculate the enrichment score of each sample, we utilized the ssGSEA method. This method calculates the grade of gene expression survival difference score inside and outside the gene set and then normalizes the enrichment score through the values obtained in all gene sets and samples[27]. This allowed us to investigate immune cell infiltration in the TME of the m6A subtype and to gain a better understanding of the underlying mechanisms of CRC.

Screening and Consensus Clustering of Differentially Expressed Genes (DEGs) Among m6A Subtypes

The "limma[17]" package in R software was used to analyze the differences of m6A methylation regulators clusters and screen the common differential genes among different genotypes. To determine significance, we considered an adjusted *p*-value of less than 0.001.

Next, we screened the genes associated with prognosis using the univariate Cox model[19], with a screening standard of *p*-value less than 0.05. To perform cluster analysis of samples, we utilized both the "limma[17]" and "ConsensusClusterPlus[20]" packages. Further, we analyzed the differences in survival status and m6A methylation regulators expression among gene clusters.

Construction of m6A-Scoring Signature and its Correlation with Mutation, Clinical, Immunotherapy, and Microsatellite Instability (MSI)

DEGs significantly related to m6A cluster prognosis were screened by univariate Cox method. We then used the principal component analysis (PCA) method to obtain the m6A score for each sample based on the expression of m6A cluster prognosis genes. This score was calculated using the formula:

$$\text{m6A score}=\sum PC1i+\sum PC2j$$

where PC1 and PC2 are the principal components obtained from the PCA analysis[28]. The optimal threshold was obtained through survival analysis. M6A cluster prognostic genes were divided into two groups. If the score was higher than the threshold, it was a high rating group, and if it was lower than the threshold, it was a low rating group. Further, we analyzed the difference in survival between these groups and conducted immune correlation analysis based on the TME-infiltrating immune cell gene set[26].

Tumor mutational burden (TMB) is a recognized biomarker of immune checkpoint inhibition response in tumors[29], which detects the mutation of every million DNA coding somatic cells[30]. We used R software to analyze the survival of tumor mutation load between high and low score groups. In addition, we also analyzed the gene mutation. According to the gene mutation, PD-L1 was selected as the target gene for differential analysis.

The differences in clinical and MSI scores between high- and low-score groups were analyzed using R software. MSI criteria were defined by comparing normal genes with those in cancer genes. When there are three base pairs mismatch, it is determined as microsatellite unstable MSI. Two or more microsatellite instability sites (MSIS) are determined as MSI-High (MSI-H), one MSI is determined as MSI-Low (MSI-L), and no MSI is determined as MSI stable (MSS)[31]. The immunotherapy scoring file was downloaded from the cancer imaging archive (TCIA) (http://tcia.at/) database, the clinical data of different CTLA-4 and PD-1 treatment effects were integrated and analyzed[32].

Statistical Analysis

The PCA method was used for the construction of the m6A score and PCA. A group of variables that may have correlation is transformed into a group of linearly uncorrelated variables through orthogonal transformation. The transformed group of variables is called principal component, which aims to reduce dimension[33]. The *k*-value selection of consensus clustering is based on the cumulative distribution function, and the proportion of *k*-value can accurately represent the overall prediction. Univariate Cox analysis was used to determine the prognostic value and the screening of m6A methylation regulator-related genes. Survival analysis used the Kaplan-Meier method to screen out patients who reached the event and terminated follow-up, and the cumulative survival probability was obtained according to the inverse survival probability[34]. A *t*-test was used to compare the two groups of data, and an analysis of variance was used to compare the three groups of data. R version 3.5.1 was used for all statistical analyses.

RESULTS

According to the screening criteria of logFC>1 and $p<0.05$, the relationship between m6A-related gene mutations and CRC was determined in the TCGA-COAD gene expression matrix and the GEO dataset GSE39582.

Genetic Variation of m6A Methylation Regulators in CRC

The mutation rate of m6A RNA methylation regulators in 399 samples was 27.82%. The results showed that ZC3H13 had the highest mutation frequency in all samples, reaching 9%. The base mutation type was mainly a cytosine mutation to thymine, and the gene mutation was mainly a missense mutation (Figure 1A). As the ZC3H13 mutation frequency was the highest, the correlation between mutation and m6A methylation regulators' expression was analyzed (Supplementary Figure 1). The ZC3H13 mutation was significantly upregulated in ALKBH5, METTL3, and RBM15; The ZC3H13 mutant was significantly downregulated in YTHDF1 and ZC3H1 ($p < 0.05$). The deletion and gain of m6A methylation regulator gene copy number were mainly concentrated on chromosomes 1-5, and the gain and deletion of m6A methylation regulator gene copy number were mainly concentrated on chromosomes 6-8 (Figure 1B).

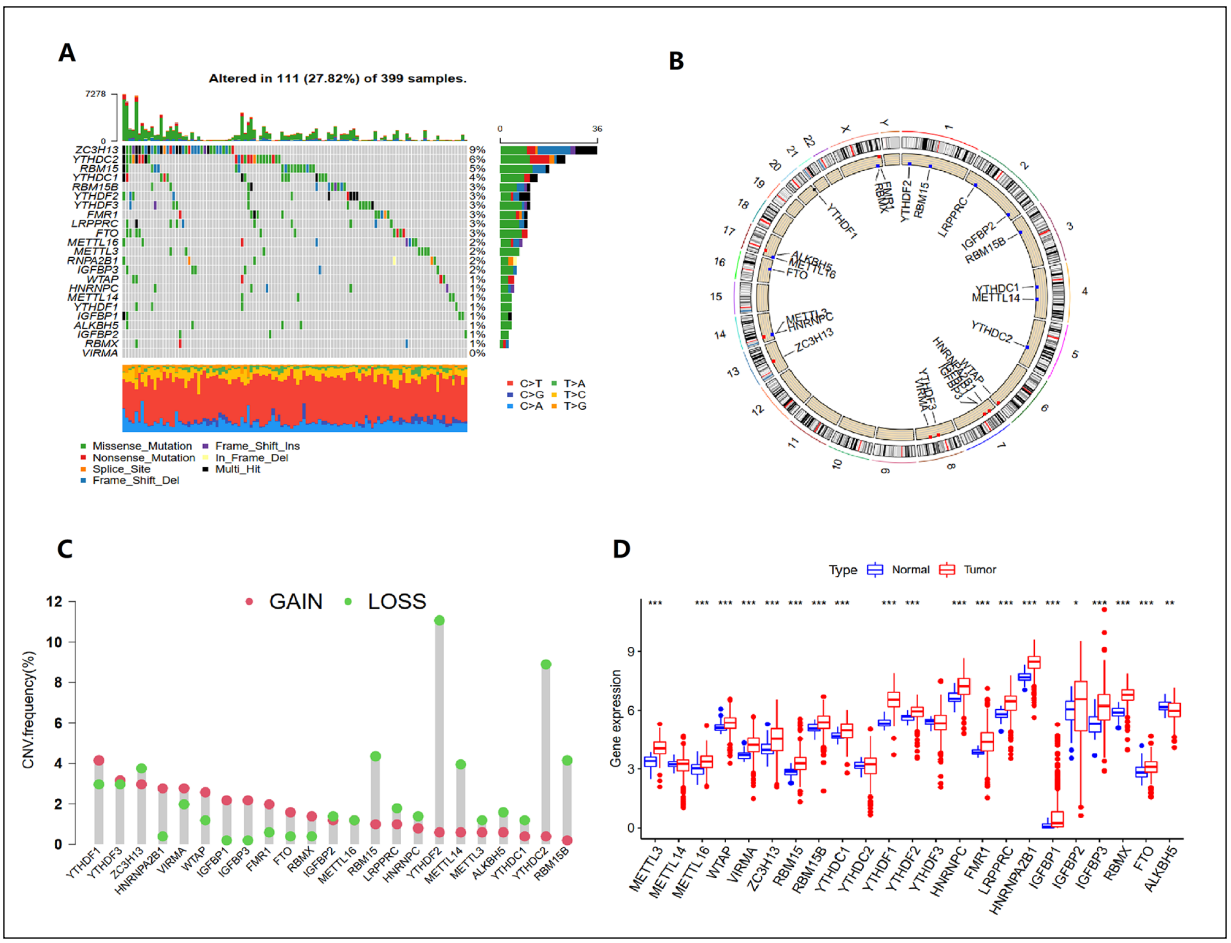

Figure 1. M6A genetic factor variation landscape in CRC (*A*) M6A RNA methylation regulator waterfall. The top is the total mutation frequency, and the left is the mutation frequency of a single gene. The middle figure shows gene mutation. Gray represents that the gene has no mutation in the sample, green represents missense mutation, red represents nonsense mutation, orange represents shear point mutation, blue represents frameshift deletion mutation, purple represents frameshift insertion mutation, and black represents multiple mutations. The lower figure shows the type of base mutation. Red represents cytosine mutation to thymine, dark blue represents cytosine mutation to guanine, blue represents cytosine mutation to adenine, green represents thymine mutation to adenine, yellow represents thymine mutation to cytosine, and orange represents thymine mutation to guanine. *B*, Copy number variation in chromosomes. The inner circle is m6A methylation regulators. The blue dot indicates that the number of deleted copies is greater than the number of increased copies, and the red dot indicates that the number of increased copies is greater than the number of deleted copies. The middle circle is the connector and the outer circle is the human chromosome. *C*, m6A methylation regulators copy number variation frequency. Red represents the increased gene copy number and green represents the missing gene copy number. *D*, Box diagram of differential analysis of 23 m6A methylation regulators in CRC. Blue is the normal sample, red is the CRC sample (***represents $p < 0.001$, **represents $p < 0.05$, *represents $p < 0.1$).

According to the m6A copy number variation frequency analysis results (Figure 1C), YTHDF1 has a significant copy number increase, and ZC3H13, RBM15, YTHDF2, METTL14, YTHDC2, RBM15B, and other genes have a significant copy number deletion. Based on the difference analysis of the TCGA database, METTL3, METTL16, WTAP, VIRMA, ZC3H13, RBM15, RBM15B, YTHDC1, YTHDF1, YTHDF2, HNRNPC, FMR1, LRPPRC, HNRNPA2B1, IGFBP1, IGFBP2, IGFBP3, RBMX, FTO, ALKBH5 were screened ($p < 0.05$), of which 18 genes had very significant differences ($p < 0.001$) (Figure 1D).

Immune Infiltration and Biological Function under m6A Methylation Modification

Univariate Cox regression analysis was used to screen m6A methylation regulators related to the prognosis of CRC (Table 2). The prognosis network diagram showed that most of the 21 m6A RNA methylation regulatory factors related to the prognosis were negatively correlated in the prognosis, and only LRPPRC, YTHPF3, YTHPF1, YTHPC2, and TGFBP2 were positively correlated in the prognosis (Figure 2A). Based on the consensus molecular clustering of 398 CRC samples in the TCGA database and 585 CRC samples in GSE39582 gene expression profile in the GEO database, according to the best stability of $k = 3$, CRC samples were divided into three subtypes (Supplementary Figure 2A-C), namely m6Acluster A, m6Acluster B and m6Acluster C. From the survival data obtained from the TCGA database and the GEO database, the shortest follow-up survival time was 0 days, and the longest was 6,030 days. Although the survival analysis showed no significant difference in survival between m6A cluster subtypes (Figure 2C), we observed differences in immune cell infiltration across m6A modification patterns. CD8(+) T cells, pre-B cells, CD4(+) T cells have high abundance in m6Acluster C. Monocytes, T helper (Th) 1 cell and neutrophilic granulocyte have high abundance in m6Acluster A. Eosinophilic granulocytes, gamma delta T cell, natural killer (NK) cell, natural killer T (NKT) cell and regulatory T cell have high abundances in m6Acluster B (Figure 2D). GSVA enrichment analysis showed differences in basic transcription factors; m6A cluster B was enriched in the ubiquitin-mediated proteolysis pathway (Supplementary Figure 3).

Table 2. Univariate analysis of the fourteen genes in the CRC patients of the TCGA cohort.

Gene symbol	Hazard ratio (95% CI)	*p*-value
IGFBP3	1.20528 (1.05987-1.37064)	0.00442
ZC3H13	1.28937 (1.04386-1.59262)	0.01836
FTO	1.39643 (1.04937-1.85828)	0.02199
LRPPRC	0.80533 (0.64612-1.00378)	0.05405
ALKBH5	1.27733 (0.93980-1.73607)	0.11795
WTAP	1.30276 (0.89914-1.88754)	0.16211
HNRNPC	1.23629 (0.91678-1.66715)	0.16440
YTHDC2	0.87938 (0.70662-1.09439)	0.24942
METTL3	1.15165 (0.87080-0.87080)	0.32220
VIRMA	1.11546 (0.86231-1.44292)	0.40542
IGFBP2	0.97188 (0.90769-1.04061)	0.41324
YTHDF1	0.91822 (0.73600-1.14556)	0.44969
YTHDF3	1.06480 (0.87995-1.28847)	0.51870
FMR1	1.02778 (0.86626-1.21942)	0.75340

Based on the three m6A modification patterns of CRC, 645 DEGs were identified (Supplementary Figure 4A). Through the analysis of biological function and pathway enrichment, m6A cluster DEGs were mainly involved in the biological processes, such as RNA splicing in BP, nuclear speck and spindle in CC, and transcription coregulator activity in MF (Figure 3A). Their functions were mainly enriched in Herpes simplex virus 1 infection and the Ubiquitin-mediated proteolysis pathway (Figure 3B). The DEGs among the three m6A clusters were identified by the univariate Cox method, and the prognosis-related genes of 118 m6A methylation regulators were obtained. A total of 967 samples from the GSE39582 gene expression profile in the TCGA and GEO databases were further clustered. According to the cumulative distri-

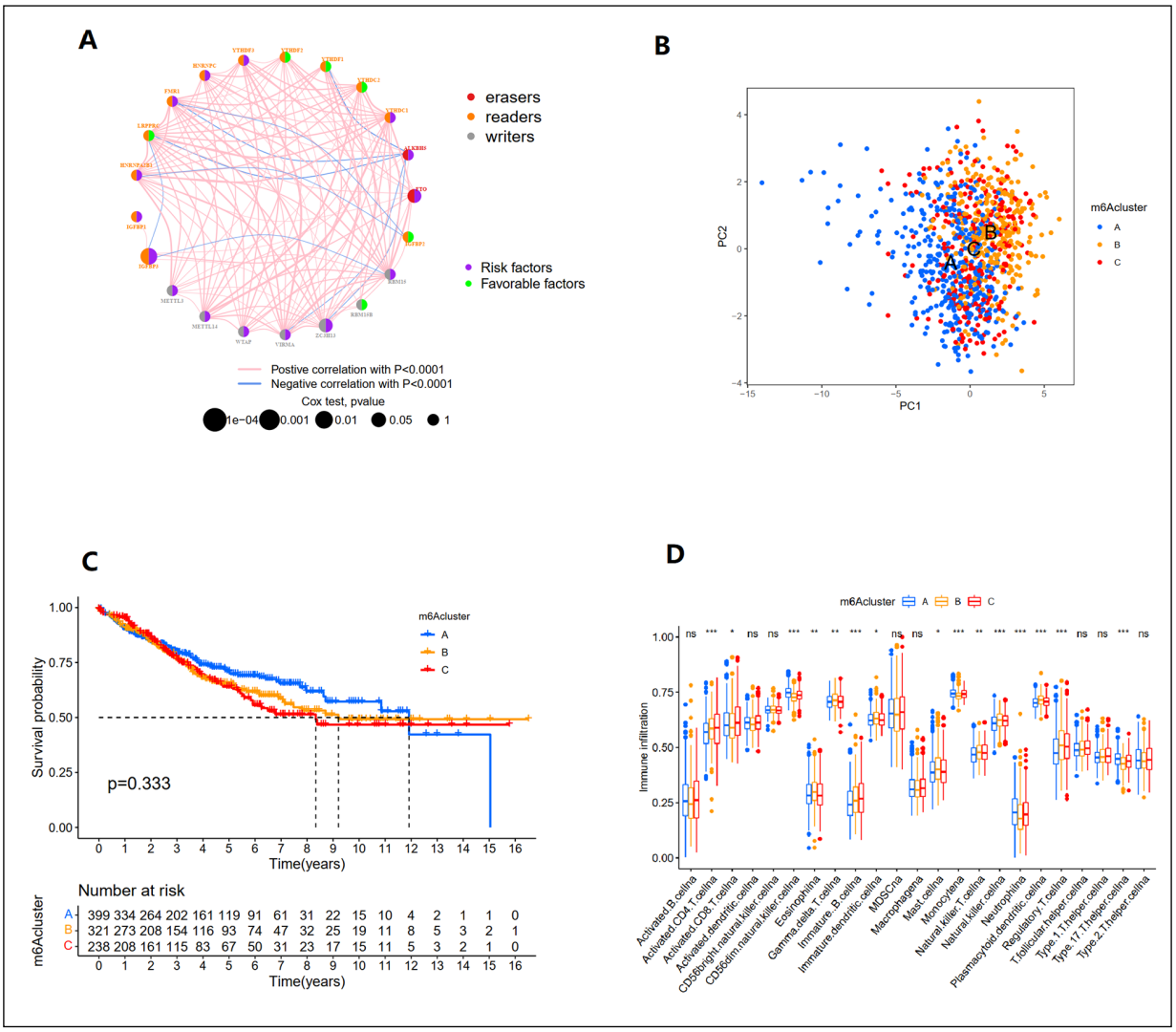

Figure 2. Interaction of m6A subtype immune infiltration (*A*) M6A RNA methylation regulators in prognosis. The red line represents a positive correlation, and the blue line represents a negative correlation. The right side of the node is gene risk, green represents low-risk gene and purple represents high-risk gene; On the left is the gene types, red for erasers, orange for readers and gray for writers. The larger the node, the more prognostic it is. *B*, m6Acluster represents type of classification, PCA1 represents principal component analysis 1, and PCA2 represents principal component analysis 2. *C*, Survival curve of m6A subtype (p = 0.333). *D*, The abscissa of the box diagram of immune cell difference analysis is immune cells, the ordinate is the content of immune cells in typing, and m6Acluster represents type of classification, *Represents difference (p < 0.1), **represents significant difference (p < 0.05), ***represents extremely significant difference (p < 0.01).

bution function, k = 3 was selected, and the CRC samples were further divided into three gene subtypes (Supplementary Figure 4B-D). Different gene subtypes showed different clinicopathological features, in which gene-cluster C was associated with m6A, cluster A and stage N0, gene-cluster B was associated with age ≤ 65 and stage N1-3, and prognosis-related genes were highly expressed in gene-cluster B and lowly expressed in gene-cluster C (Supplementary Figure 4E). By analyzing the survival of the three gene subtypes, we found that as time increased, the survival rate of patients decreased, and there were significant differences in survival among the three gene subtypes. The prognosis of gene-cluster B was the worst, that of gene-cluster C was the best, and the five-year survival rate of each subtype was higher than 50% (Figure 3C). The difference analysis of 21 m6A methylation regulators in gene subtypes showed that the expression of 19 m6A methylation regulators was different in different gene subtypes. We observed that, except for IGFBP2 and ALKBH5, which were highly expressed in gene-cluster C, the rest were highly expressed in gene-cluster A and gene-cluster B (Figure 3D).

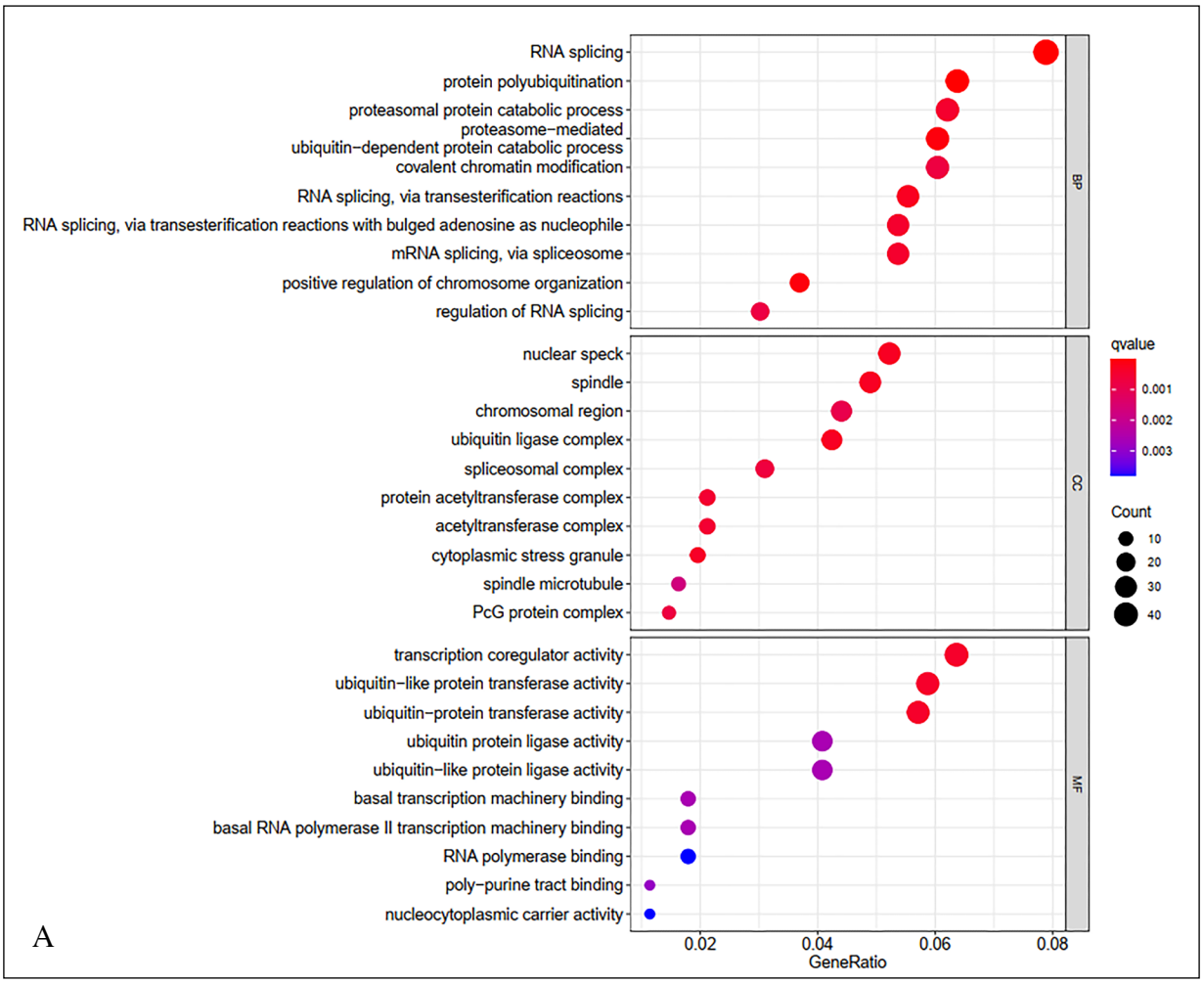

Figure 3. Biological function annotation and genomic characteristics. *A*, GO function enrichment analysis point diagram. BP represents molecular function; CC represents biological process and MF represents cell composition. The point is from small to large, and the color is from blue to red, representing the enrichment degree from low to high.

Continued

Construction of m6A-Scoring Signature

In order to more accurately analyze the changes of m6A modification pattern in CRC patients, we constructed a scoring system to judge the changes of m6A modification pattern in each CRC patient. 958 CRC samples in the TCGA and GEO databases were divided into high rating group and low rating group. The results of the survival analysis showed a very significant difference in survival between the high- and low-score groups ($p < 0.001$), with better survival in the high-score group (Figure 4A). TMB analysis demonstrated a significant survival difference between the high and low score groups ($p = 0.04$) (Figure 4B). The Sankey Diagram shows the changes of the m6A cluster, gene cluster, high and low rating groups, survival status, and other attributes of a single patient. The number of survivors in the high rating group is higher than that in the low rating group, and gene clusters A and C belong to the high-score group (Figure 4C). We analyzed the tumor somatic mutations in the m6A high-score group and the m6A low-score group. In the m6A scoring group, the mutation probability of APC was the highest (76 *vs.*73%), followed by the lower TP53 (57% *vs*. 65%) (Figure 4D and 4E). There was a significant difference in m6A score between m6A cluster A and B ($p<0.05$), with the highest score in m6A cluster A and the lowest score in m6A cluster B (Figure 4F). There was a significant difference in m6A score among gene clusters ($p<0.05$). The score was the highest in gene-cluster C and the lowest in m6A cluster B (Figure 4G).

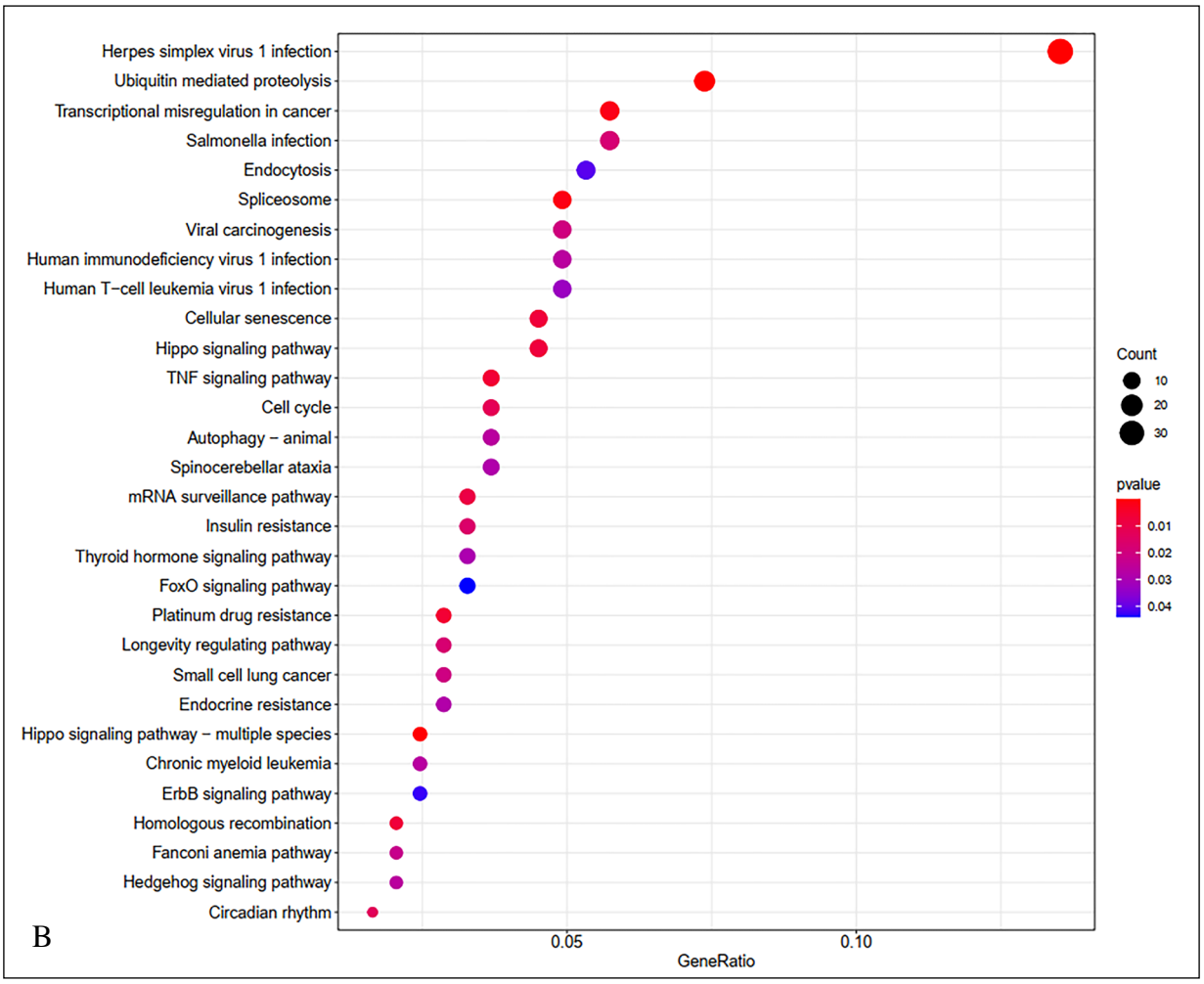

Figure 3 *(continued)*. *B*, KEGG pathway enrichment analysis point map. Dot from small to large, color from blue to red, representing the enrichment degree from low to high.

Continued

Clinical correlation analysis showed that there was a significant difference in the m6A score in survival status, and the m6A score was higher in the survival group (Figure 4H). The results of survival analysis showed that the m6A score was closely related to clinical traits. There was a significant difference in the m6A score among patients at the T3-T4 stage. The survival of the high-grade group was better than that of the low-grade group (Supplementary Figure 5). The independent prognostic analysis included age, sex, T stage, and N stage. The results showed that the m6A score was an independent prognostic factor for CRC ($p < 0.05$), and T stage and N stage could also be used as independent prognostic factors for CRC ($p < 0.05$, Figure 4I and 4J).

Unique Immunotherapy Landscape of m6A Score

M6A score is closely related to many immune cell infiltrations. In the immune correlation analysis, m6A score was significantly negatively correlated with eosinophilic granulocytes, pre-B cell, immature dendritic cell, myeloid-derived suppressor cell (MDSC), macrophages, mast cell, NKT cell, natural killer cell, T follicular helper cell, T helper (Th) 1 cell, and significantly positively correlated with CD56(dim) NK cell, T helper (Th) 17 cell (Figure 5A).

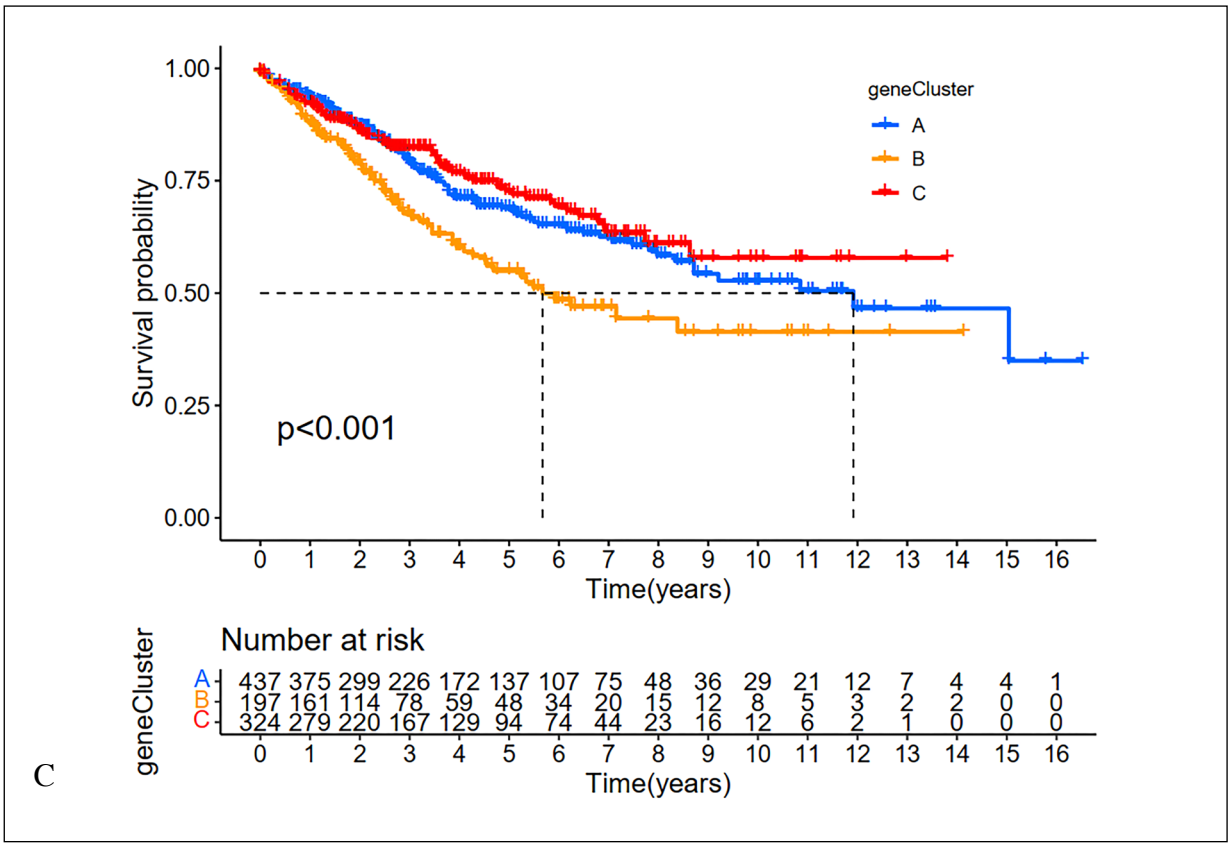

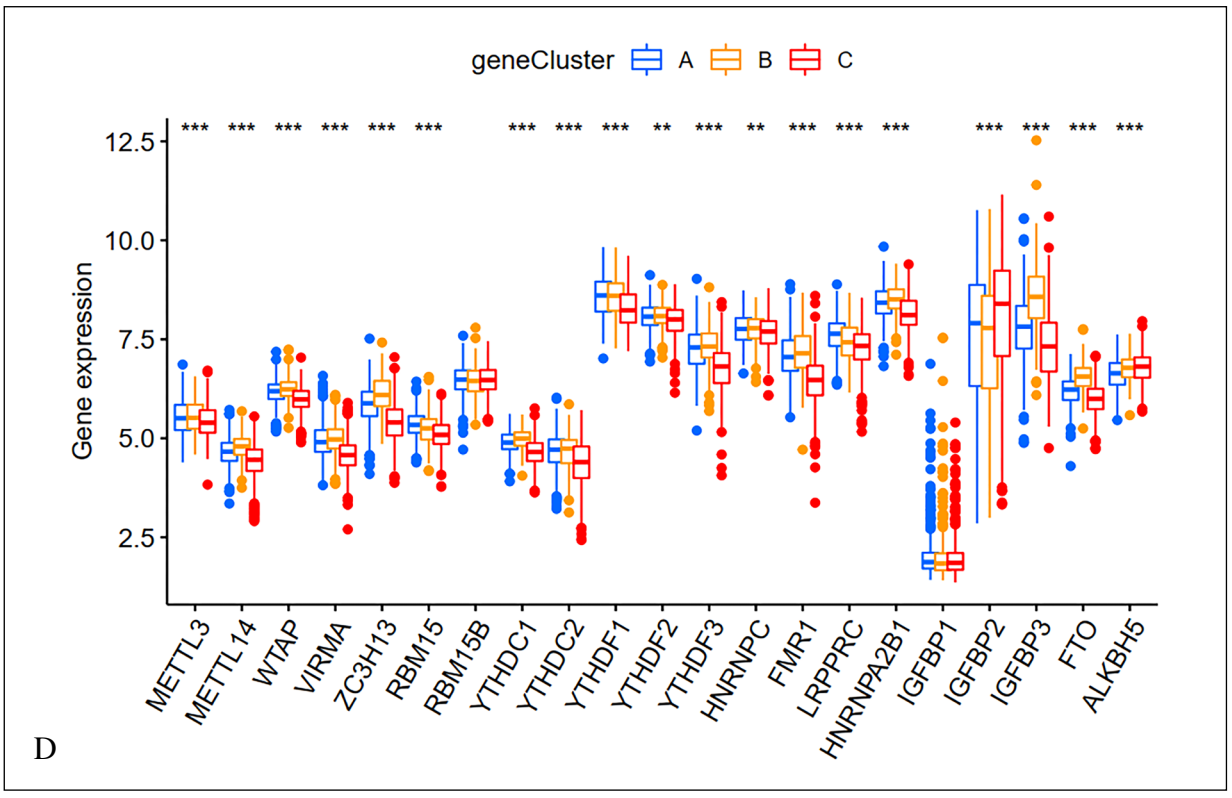

Figure 3 *(continued)*. *C*, Survival curve of genotyping ($p < 0.001$). *D*, The box diagram of m6A difference analysis of gene cluster, the abscissa is m6A methylation regulators, the ordinate is the expression of m6A methylation regulators in gene cluster, and genecluster represents genotyping type, *stands for difference ($p < 0.1$), **stands for significant difference ($p < 0.05$), ***stands for very significant difference ($p < 0.001$), NS stands for no significant.

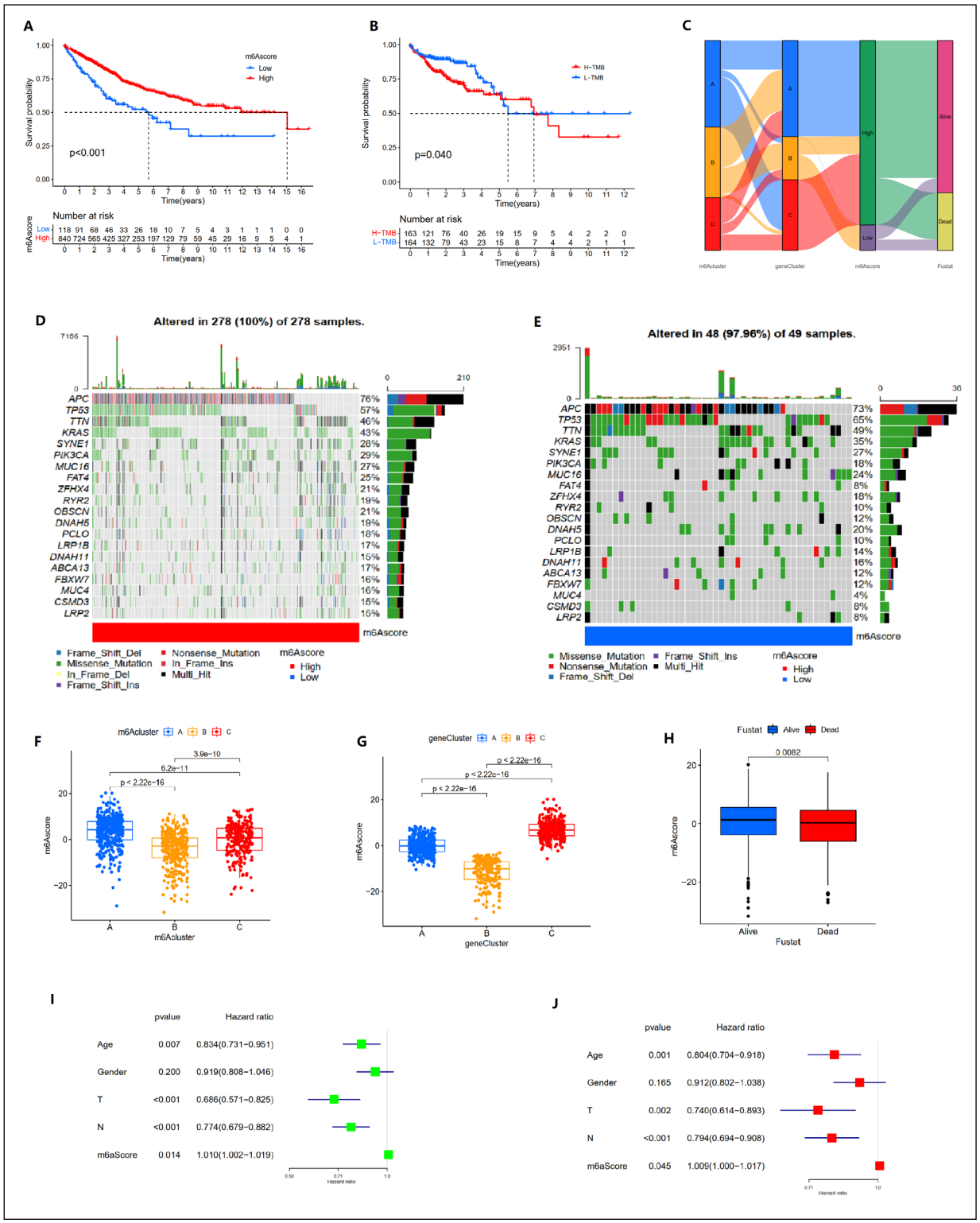

Figure 4. *A*, Survival curve of m6A score ($p < 0.001$). *B*, Tumor mutation load survival curve ($p = 0.04$). *C*, Sankey Diagram of different m6A cluster and gene cluster. *D*, Gene mutation waterfall of m6A high-score group. *E*, Gene mutation waterfall of m6A low-score group. *F*, Analysis of m6A score difference in m6A cluster. *G*, Difference analysis of m6A score in gene cluster. *H*, M6A score was correlated with survival status, and there was significant difference between survival status in m6A score ($p = 0.0082$). *I*, Forest diagram of univariate independent prognostic analysis of m6A score and clinical characters. *J*, Forest diagram of multivariate independent prognostic analysis of m6A score and clinical characters.

The progress of immune checkpoints has also attracted much attention. We analyzed the immune checkpoints PD-L1 and CTLA-4. The difference analysis results showed that PD-L1 and CTLA-4 had a significant difference in m6A score ($p < 0.05$), and the expression was higher in the low evaluation group (Figure 5B and 5C). Because the clinical characteristics of the high m6A-score group are better than those of the low m6A-score group, and the close relationship between m6A score and immune cell infiltration, we further discussed the response to immune checkpoint inhibitor (ICI) treatment represented by CTLA-4/PD-1 inhibitors in terms of immunotherapy. The analysis results showed that there were differences in immunotherapy between the high and low m6A-score groups ($p < 0.05$), and the high m6A-score group received anti-CTLA4 and anti-PD1 alone, which had a good effect (Figure 5D and 5E). In addition, MSI was also analyzed; the vast majority of the high m6A-score group belonged to the MSS category, and the proportion of microsatellite instability (MSI-L) cases was the same for the two groups (Figure 5H). MSI did not differ in m6A scores (Figure 5I). The above results showed that the m6A score was significantly correlated with the immune response.

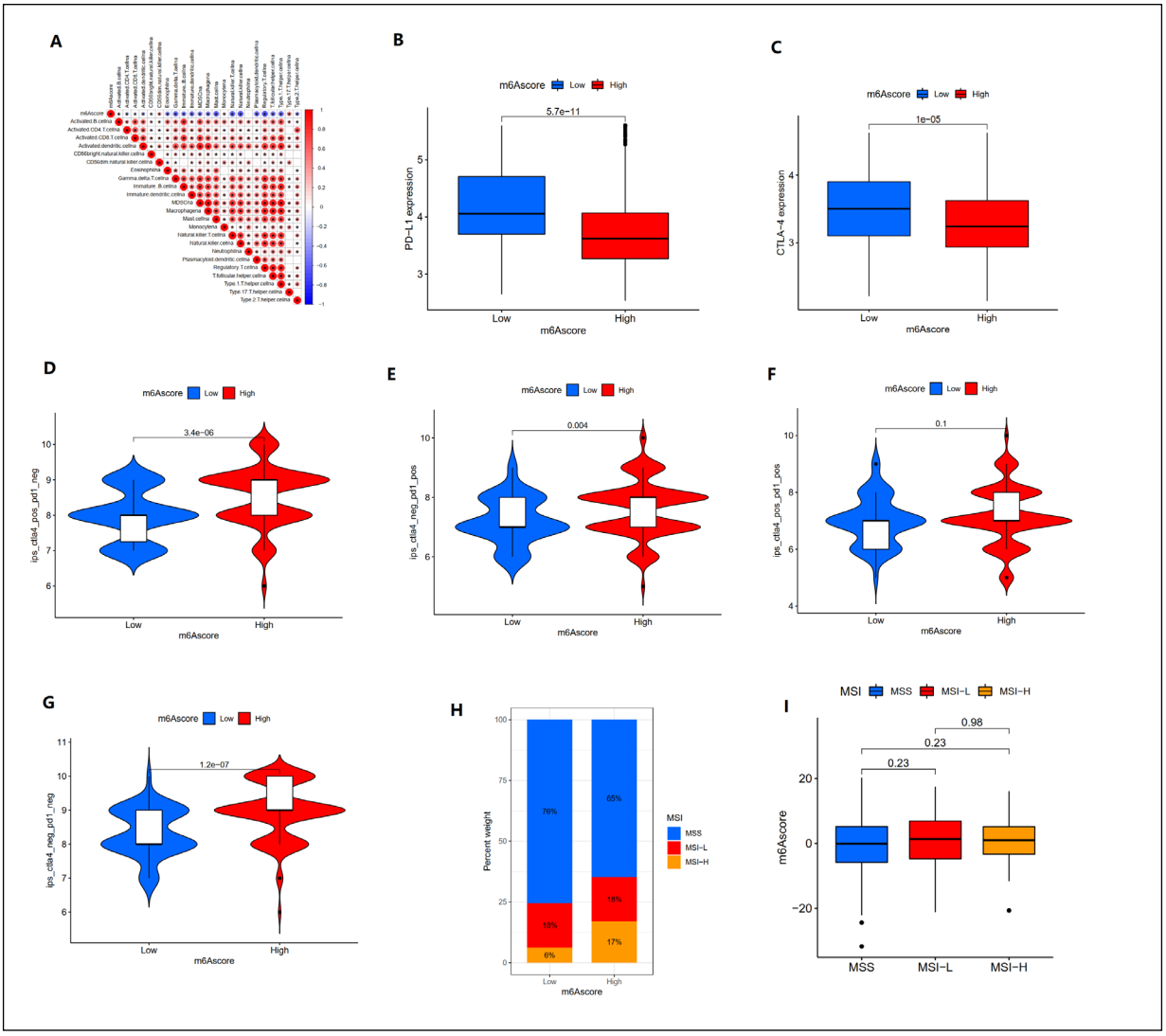

Figure 5. Characteristics of m6A score in immune response. *A*, Correlation analysis between immune cells and m6A score. Red is positive correlation, blue is negative correlation, and * is significant correlation. *B*, Difference analysis of PD-L1 expression between m6A scores (p = 5.7e-11). *C*, Difference analysis of CTLA-4 expression between m6A scores (p = 1e-05). *D-G*, M6A modification pattern in anti-PD-L1 and anti-CTLA-4 immunotherapy. Figure *D* is Violin of m6A score and anti-CTLA-4 immunotherapy (p = 3.4e-06), figure *E* is Violin of m6A score and anti-PD-1 immunotherapy (p = 0.004), figure *F* is Violin of m6A score and anti-PD-1 combined with CTLA-4 immunotherapy (p = 0.1), and figure *G* is Violin of m6A score and non-anti-PD-1 combined with CTLA-4 immunotherapy Violin (p = 1.2e-07). *H*, M6A score and MSI histogram. *I*, M6A score difference between MSI (MSS vs.MSI-L: p = 0.23, MSS vs.MSI-H: p = 0.23, MSI-L vs.MSI-H: p = 0.96).

DISCUSSION

M6A modification of m6A methylation regulators also plays an important role in clinical, TME, and immune response[35]. In this study, we first summarized the action mode and mechanism of m6A RNA methylation regulators in cancer, determined three methylation modification modes according to 23 m6A methylation regulators, and explored their correlation with clinicopathological features and TME infiltration, so as to obtain potential prognostic features, which is helpful to the formulation of immunotherapy strategies for CRC.

We divided the samples into three m6A subtypes by consensus clustering. Clinically, m6Acluster A was significantly associated with older age, whereas m6Acluster C was significantly associated with N0 stage and showed an activated phenotype. CD4(+) T cell, CD56(dim) NK cell, pre-B cell, monocytes, NK cell, neutrophilic granulocyte, plasmacytoid dendritic cell, regulatory T cell, T helper (Th) 1 cell, and other immune cells showed significant differences in different m6A subtypes. m6A cluster A is characterized by enrichment of monocytes, which is consistent with the immune desert phenotype[36]. m6Acluster B is characterized by lack of T cells, enrichment of participation in ubiquitin mediated proteolysis, which is consistent with immune depleted phenotype[36]. m6A cluster C is characterized by CD4+ T cell enrichment, which is consistent with the immune-excluded phenotype[36]. Neutrophilic granulocyte plays an anti-tumor or tumor-promoting role in a microenvironment-related manner. It shows a very significant difference and low relative content in malignant tumors such as lung adenocarcinoma[37], primary GBM[38], and renal clear cell carcinoma[39]. CD4+ T cells often play an immunosuppressive role in cancer to promote tumor[40]. It was found that CD4+ T cells accumulated continuously in the TME of CRC patients and were immunosuppressed in combination with IL-10 and TGF-β[41]. This indicates that m6A methylation modification pattern is significantly associated with immune activation and other pathways.

Further cluster analysis was carried out according to the transcriptional expression pattern, and three gene subtypes were obtained. IGFBP3, FMR, and HNRNPA2B1 were the most expressed in gene-cluster B. METTL3, METTL14, WTAP, VIRMA, ZC3H13, RBM15, FTO, YTHDC1, and YTHDC were the lowest in gene-cluster C. It was found that HNRNPA2B1, as a reader modified by m6A methylation, was identified as an oncogene in head and neck cancer (HNC) because its overexpression can promote the epithelial-mesenchymal transformation of HNC cells[42]. It has also been reported that the increased expression of HNRNPA2B1 is related to risk and prognosis. Knocking down HNRNPA2B1 can accelerate apoptosis[43]. HNRNPA2B1 is regulated by long non-coding RNA H19 in CRC, and the combination of the two will promote the occurrence of cancer[44]. However, in ovarian cancer (OC), the prognosis of OC patients with low expression of VIRMA or high expression of HNRNPA2B1 is better than that of the control group, which confirms that VIRMA is a risk prognostic gene in OC and HNRNPA2B1 is a protective prognostic gene[45]. The main role of VIRMA is mediating mRNA m6A methylation in the 3 'UTR and near stop codon[46], which regulates the expression of Oncogene lncRNA in prostate cancer (PCa). The high expression leads to a shortened disease-free survival time, resulting in poor prognosis and a significant correlation with the recurrence of prostatic adenocarcinoma[47]. FTO, also known as ALKBH9, is a member of the Fe(II)/2-oxoglutarate-dependent dioxygenase AlkB family[48]. In CRC, the expression of FTO is the lowest in gene-cluster C with the best prognosis. Similarly, the group with high expression of GC FTO in gastric cancer also has a worse prognosis[49]. However, its low expression in bladder cancer (BC) can promote cancer cell metastasis and proliferation[50]. Through the study, we found that there were great differences in survival among gene clusters. The survival of gene-cluster B was worse than that of gene-cluster A and C, which could reliably predict the survival of patients. In order to more conveniently explore the relationship between m6A modification mode and CRC TME, clinic, and immunity, we constructed the m6A-score system and analyzed the prognosis, clinic, immunity, and TME of m6A modification mode.

We found the correlation between the m6A score and prognosis and immune cells. M6A score is negatively correlated with most immune cell types, but it has been proven to be a favorable prognostic factor in many reports on the relationship between immune cells and CRC survival rate[51]. This contradictory result suggests that the m6A score may reflect the quality and functional orientation of the immune infiltrate rather than its raw quantity. One possible biological mechanism is that a high m6A score delineates a tumor microenvironment that is less immunosuppressive. Specifically, our analysis showed that the m6A score was negatively correlated with cell types known for their roles in suppressing anti-tumor immunity, such as myeloid-derived suppressor cells (MDSCs), macrophages, and regulatory T cells. Conversely, it was positively correlated with cell types like CD56(dim) NK cells and T helper 17 (Th17) cells, which can mediate potent anti-tumor effects. Therefore, a high m6A score might signify a shift away from a dense but ineffective or suppressed immune environment towards one that is less infiltrated but more functionally potent and anti-tumorigenic. Furthermore, this hypothesis is consistent with our

findings on immune checkpoints. The significantly lower expression of PD-L1 and CTLA-4 in the high-score group indicates a less exhausted immune state. A less exhausted T-cell population would be more effective at controlling the tumor, thus explaining both the better prognosis and the enhanced response to anti-CTLA-4 and anti-PD-1 therapies.

Although there was no significant difference in TMB in CRC, the gene mutation rate was at a high level. There was a significant difference in the expression of PD-L1 in m6A score. Immunotherapy also achieved a better prediction effect in the high evaluation group. M6A score is the highest in m6Acluster A, the highest in gene-cluster C, and the lowest in m6Acluster B and gene-cluster B. Combined with the clinical characteristics of m6A score, we can classify CRC patients according to m6A subtype characteristics and gene subtype characteristics. M6A score was positively correlated with high-level infiltrated $CD56^{+}$ natural killer (NK) cells, monocytes, and T helper type 17 cells (Th17), which was consistent with the results of previous studies. Previous studies have shown that $CD16^{+}$/CD56 + NK can effectively predict the prognosis of patients after chemotherapy[52]. In addition, it has been reported that Th17 can play an auxiliary role in VEGF antibody treatment and effectively improve the sensitivity of tumors to VEGF antibody[53]. M6A score also has the characteristics of a gene and a somatic mutation. In CRC samples, APC has a higher mutation rate in the high-evaluation group, whereas TP53 has a higher mutation rate in the low-evaluation group. m6A cluster B is enriched in the ubiquitin-mediated protein hydrolysis pathway, which is closely related to the high mutation rate of APC. APC/C-Cdc20 is the main switch and regulator of mitosis, which acts on the ubiquitination of downstream targets under the control of phosphorylation and specific inhibitors[54]. APC mutation accumulation has been proven to lead to tumorigenesis in CRC[55].

The M6A score also shows significant associations with clinical features and immune checkpoints in immunotherapy. The study indicates that the high evaluation group has a greater survival rate. Although this feature has no guiding significance in the T1-T2 stage, it is very significant in the T3-T4 stage. Our study shows that the m6A score can be used as an independent prognostic factor in patients with CRC. Previous studies have also demonstrated that the m6A score has certain guiding significance in prognosis. The m6A score characteristics constructed by Zhu et al[56] can be an independent prognostic feature of BC patients (HR = 1.198, 95% CI: 1.031-1.390), and the high-score group has a better prognosis than the low-score group. We also found that anti-CTLA-4 and anti-PD-1 immunotherapy alone were more effective in the high evaluation group, while programmed cell death 1 ligand 1 (PD-L1) had higher expression in the low evaluation group. Huang et al[57] also predicted the effect of immunotherapy in hepatocellular carcinoma through m6A score characteristics, in which immunotherapy was better in high evaluation groups. The findings can be applied to the auxiliary evaluation of chemotherapy efficacy and clinical response. However, whether m6A score characteristics can predict the prognosis of patients after chemotherapy needs further research. PD-L1 was also found to be significantly correlated with low m6A-score in breast cancer (BRCA)[58], which may have a certain impact on the efficacy of immunotherapy. At present, our research has some limitations. First, M6A modification mode involves not only 23 mRNA methylation regulators, but also TME. TME is a complex entity with dynamic crosstalk among cancer, the matrix, and immunity. The analysis only focusing on immune cells and immune genes is not comprehensive. Second, it is unclear whether the m6A modification mode is suitable for patients after treatment. Third, this study is entirely based on computational analyses of public datasets (TCGA and GEO) and lacks experimental validation and verification in independent clinical cohorts. We identified key findings such as high mutation frequency of ZC3H13, distinct immune infiltration characteristics of three m6A clusters, and the predictive value of m6A score for immunotherapy response, but these observations have not been confirmed by wet-lab experiments. For instance, we have not used RT-qPCR to validate the differential expression of core m6A regulators (e.g., ZC3H13, METTL3) between CRC tumor and normal tissues, nor have we applied IHC to verify the correlation between m6A subtypes and TME infiltration markers (e.g., CD4+ T cells, MDSCs). Additionally, the prognostic and therapeutic significance of the m6A score has not been tested in an independent clinical sample set outside the existing public datasets. This limitation restricts the immediate translational impact of our findings, as computational results—while hypothesis-generating—require experimental corroboration to support their reliability in clinical practice.

CONCLUSIONS

In this study, we comprehensively evaluated the m6A modification patterns of 23 m6A methylation regulators. The differences in m6A modification patterns may be an important factor in the heterogeneity and complexity of TME. Evaluating the modification pattern of m6A in a single CRC will enhance our understanding of the infiltration characteristics of TME and provide a basis for guiding immunotherapy strategies.

Acknowledgements:
Not applicable.

Funding:
This study was funded by the Double First-Class University Plan (MOE, China Ministry of Education) and the Minzu University 985 Academic Team-building Fund (No. 2024MDTD25C) and the Beijing Municipal Science and Technology Commission.

Availability of Data and Materials:
Publicly available datasets were analyzed in this study. This data can be found here: https://www.ncbi.nlm.nih.gov/geo/, http://cancergenome.nih.gov/, www.gsea-msigdb.org/gsea/index.jsp, http://tcia.at/. The data generated in the present study may be requested from the corresponding author.

Authors' Contributions:
WW and HW contributed equally to this work. WW, HW, and TM collected, analyzed, interpreted the data, and drafted the manuscript. TM and YH conceived and designed the study, had full access to all data, and took responsibility for the integrity and accuracy of the data analysis. YZ participated in revising the manuscript. All authors read and approved the final version of the manuscript.

ORCID ID:
Wenqi Wang: 0009-0000-9948-5981
Zhaohua Wang: 0009-0008-1778-1196
Yupei Zhan: 0009-0006-8930-8897
Yunfei Gao: 0009-0003-2914-7612
Tianxiao Ma: 0000-0002-4680-1722
Yaojiang Huang: 0000-0001-5409-5605

Ethics approval:
Not applicable.

Patient consent for publication:
Not applicable.

Conflict of interest:
The authors declare that they have no competing interests.

REFERENCES

1. Weitz J, Koch M, Debus J, Höhler T, Galle PR, Büchler MW. Colorectal cancer. Lancet 2005; 365: 153-165.
2. Siegel RL, Miller KD, Jemal A. Cancer statistics, 2020. CA Cancer J Clin 2020; 70: 7-30.
3. Guillem JG, Puig-La Calle J Jr, Cellini C, Murray M, Ng J, Fazzari M, Paty PB, Quan SH, Wong WD, Cohen AM. Varying features of early age-of-onset "sporadic" and hereditary nonpolyposis colorectal cancer patients. Dis Colon Rectum 1999; 42: 36-42.
4. Liu ZX, Li LM, Sun HL, Liu SM. Link Between m6A Modification and Cancers. Front Bioeng Biotechnol 2018; 6: 89.
5. Shen S, Zhang R, Jiang Y, Li Y, Lin L, Liu Z, Zhao Y, Shen H, Hu Z, Wei Y, Chen F. Comprehensive analyses of m6A regulators and interactive coding and non-coding RNAs across 32 cancer types. Mol Cancer 2021; 20: 67.
6. Ma X, Li Y, Wen J, Zhao Y. m6A RNA methylation regulators contribute to malignant development and have a clinical prognostic effect on cervical cancer. Am J Transl Res 2020; 12: 8137-8146.
7. Liao Y, Han P, Zhang Y, Ni B. Physio-pathological effects of m6A modification and its potential contribution to melanoma. Clin Transl Oncol 2021; 23: 2269-2279.
8. Chen M, Wong CM. The emerging roles of N6-methyladenosine (m6A) deregulation in liver carcinogenesis. Mol Cancer 2020; 19: 44.
9. Fröhling S, Scholl C, Gilliland DG, Levine RL. Genetics of myeloid malignancies: pathogenetic and clinical implications. J Clin Oncol 2005; 23: 6285-6295.
10. Lin S, Choe J, Du P, Triboulet R, Gregory RI. The m(6)A Methyltransferase METTL3 Promotes Translation in Human Cancer Cells. Mol Cell 2016; 62: 335-345.
11. Zhu W, Si Y, Xu J, Lin Y, Wang JZ, Cao M, Sun S, Ding Q, Zhu L, Wei JF. Methyltransferase like 3 promotes colorectal cancer proliferation by stabilizing CCNE1 mRNA in an m6A-dependent manner. J Cell Mol Med 2020; 24: 3521-3533.
12. Hanahan D, Weinberg RA. Hallmarks of cancer: the next generation. Cell 2011; 144: 646-674.

13. Li G, Qin Z, Chen Z, Xie L, Wang R, Zhao H. Tumor Microenvironment in Treatment of Glioma. Open Med (Wars) 2017; 12: 247-251.
14. Wang F, Malnassy G, Qiu W. The Epigenetic Regulation of Microenvironment in Hepatocellular Carcinoma. Front Oncol 2021; 11: 653037.
15. Liu Y, Yuan Y, Zhou Z, Jiang X, He S, Wei F, Cui Y, Yang L, Zhao G. Mettl14 sustains FOXP3 expression to promote the differentiation and functions of induced-regulatory T cells via the mTOR signaling pathway. Immunology Letters 2023; 258: 35-44.
16. Feng L, Li M, Ma J, Wang W, Wang S, Mao Z, Zhang Y. ALKBH5 regulates arginase 1 expression in MDSCs and their immunosuppressive activity in tumor-bearing host. Noncoding RNA Res 2024; 9: 913-920.
17. Ritchie ME, Phipson B, Wu D, Hu Y, Law CW, Shi W, Smyth GK. limma powers differential expression analyses for RNA-sequencing and microarray studies. Nucleic Acids Res 2015; 43: e47.
18. Marisa L, de Reyniès A, Duval A, Selves J, Gaub MP, Vescovo L, Etienne-Grimaldi MC, Schiappa R, Guenot D, Ayadi M, Kirzin S, Chazal M, Fléjou JF, Benchimol D, Berger A, Lagarde A, Pencreach E, Piard F, Elias D, Parc Y, Olschwang S, Milano G, Laurent-Puig P, Boige V. Gene expression classification of colon cancer into molecular subtypes: characterization, validation, and prognostic value. PLoS Med 2013; 10: e1001453.
19. Zhang S, Li J, Gao H, Tong Y, Li P, Wang Y, Du L, Wang C. lncRNA Profiles Enable Prognosis Prediction and Subtyping for Esophageal Squamous Cell Carcinoma. Front Cell Dev Biol 2021; 9: 656554.
20. Wilkerson MD, Hayes DN. ConsensusClusterPlus: a class discovery tool with confidence assessments and item tracking. Bioinformatics 2010; 26: 1572–1573.
21. Liu P, Jiang W, Zhao J, Zhang H. Integrated analysis of genome-wide gene expression and DNA methylation microarray of diffuse large B-cell lymphoma with TET mutations. Mol Med Rep 2017; 16: 3777-3782.
22. Hänzelmann S, Castelo R, Guinney J. GSVA: gene set variation analysis for microarray and RNA-seq data. BMC Bioinformatics 2013; 14: 7.
23. Yu G, Wang LG, Han Y, He QY. clusterProfiler: an R package for comparing biological themes among gene clusters. OMICS 2012; 16: 284-287.
24. Yu G, Wang LG, Yan GR, He QY. DOSE: an R/Bioconductor package for disease ontology semantic and enrichment analysis. Bioinformatics 2015; 31: 608-609.
25. Deng Y, Xie Q, Zhang G, Li S, Wu Z, Ma Z, He X, Gao Y, Wang Y, Kang X, Wang J. Slow skeletal muscle troponin T, titin and myosin light chain 3 are candidate prognostic biomarkers for Ewing's sarcoma. Oncol Lett 2019; 18: 6431-6442.
26. Santegoets SJ, van Ham VJ, Ehsan I, Charoentong P, Duurland CL, van Unen V, Höllt T, van der Velden LA, van Egmond SL, Kortekaas KE, de Vos van Steenwijk PJ, van Poelgeest MIE, Welters MJP, van der Burg SH. The Anatomical Location Shapes the Immune Infiltrate in Tumors of Same Etiology and Affects Survival. Clin Cancer Res 2019; 25: 240-252.
27. Barbie DA, Tamayo P, Boehm JS, Kim SY, Moody SE, Dunn IF, Schinzel AC, Sandy P, Meylan E, Scholl C, Fröhling S, Chan EM, Sos ML, Michel K, Mermel C, Silver SJ, Weir BA, Reiling JH, Sheng Q, Gupta PB, Wadlow RC, Le H, Hoersch S, Wittner BS, Ramaswamy S, Livingston DM, Sabatini DM, Meyerson M, Thomas RK, Lander ES, Mesirov JP, Root DE, Gilliland DG, Jacks T, Hahn WC. Systematic RNA interference reveals that oncogenic KRAS-driven cancers require TBK1. Nature 2009; 462: 108-112.
28. Meng J, Huang X, Qiu Y, Yu M, Lu J, Yao J. Characterization of m6A-Related Genes Landscape in Skin Cutaneous Melanoma to Aid Immunotherapy and Assess Prognosis. Int J Gen Med 2021; 14: 5345-5361.
29. Sung WWY, Chow JCH, Cho WCS. Tumor mutational burden as a tissue-agnostic biomarker for cancer immunotherapy. Expert Rev Clin Pharmacol 2021; 14: 141-143.
30. Yarchoan M, Hopkins A, Jaffee EM. Tumor Mutational Burden and Response Rate to PD-1 Inhibition. N Engl J Med 2017; 377: 2500-2501.
31. Wu S, Liu X, Wang J, Zhou W, Guan M, Liu Y, Pang J, Lu T, Zhou L, Shi X, Wu H, Liang Z, Zeng X. DNA Mismatch Repair Deficiency Detection in Colorectal Cancer by a New Microsatellite Instability Analysis System. Interdiscip Sci 2020; 12: 145-154.
32. Zhang B, Wu Q, Li B, Wang D, Wang L, Zhou YL. m6A regulator-mediated methylation modification patterns and tumor microenvironment infiltration characterization in gastric cancer. Mol Cancer 2020; 19: 53.
33. Gewers FL, Ferreira GR, De Arruda HF, Silva FN, Comin CH, Amancio DR, Costa LD. Principal component analysis: A natural approach to data exploration. ACM Comput Surv 2021; 54: 1-34.
34. Koletsi D, Pandis N. Survival analysis, part 2: Kaplan-Meier method and the log-rank test. Am J Orthod Dentofacial Orthop 2017; 152: 569-571.
35. Cong R, Ji C, Zhang J, Zhang Q, Zhou X, Yao L, Luan J, Meng X, Song N. m6A RNA methylation regulators play an important role in the prognosis of patients with testicular germ cell tumor. Transl Androl Urol 2021; 10: 662-679.
36. Chen DS, Mellman I. Elements of cancer immunity and the cancer-immune set point. Nature 2017; 541: 321-330.
37. Zhou H, Zheng M, Shi M, Wang J, Huang Z, Zhang H, Zhou Y, Shi J. Characteristic of molecular subtypes in lung adenocarcinoma based on m6A RNA methylation modification and immune microenvironment. BMC Cancer 2021; 21: 938.
38. Cai Z, Zhang J, Liu Z, Su J, Xu J, Li Z, Meng H, Zhang H, Huang M, Zhao D, Duan C, He X. Identification of an N6-methyladenosine (m6A)-related signature associated with clinical prognosis, immune response, and chemotherapy in primary glioblastomas. Ann Transl Med 2021; 9: 1241.
39. Li H, Hu J, Yu A, Othmane B, Guo T, Liu J, Cheng C, Chen J, Zu X. RNA Modification of N6-Methyladenosine Predicts Immune Phenotypes and Therapeutic Opportunities in Kidney Renal Clear Cell Carcinoma. Front Oncol 2021; 11: 642159.
40. Borst J, Ahrends T, Bąbała N, Melief CJM, Kastenmüller W. CD4+ T cell help in cancer immunology and immunotherapy. Nat Rev Immunol 2018; 18: 635-647.
41. Zhong W, Jiang ZY, Zhang L, Huang JH, Wang SJ, Liao C, Cai B, Chen LS, Zhang S, Guo Y, Cao YF, Gao F. Role of LAP+CD4+ T cells in the tumor microenvironment of colorectal cancer. World J Gastroenterol 2017; 23: 455-463.
42. Gupta A, Yadav S, Pt A, Mishra J, Samaiya A, Panday RK, Shukla S. The HNRNPA2B1-MST1R-Akt axis contributes to epithelial-to-mesenchymal transition in head and neck cancer. Lab Invest 2020; 100: 1589-1601.
43. Yang Y, Wei Q, Tang Y, Yuanyuan Wang, Luo Q, Zhao H, He M, Wang H, Zeng Q, Lu W, Xu J, Liu T, Yi P. Loss of hnRNPA2B1 inhibits malignant capability and promotes apoptosis via down-regulating Lin28B expression in ovarian cancer. Cancer Lett 2020; 475: 43-52.

44. Zhang Y, Huang W, Yuan Y, Li J, Wu J, Yu J, He Y, Wei Z, Zhang C. Long non-coding RNA H19 promotes colorectal cancer metastasis via binding to hnRNPA2B1. J Exp Clin Cancer Res 2020; 39: 141. Erratum in: J Exp Clin Cancer Res 2021; 40: 111.
45. Li Q, Ren CC, Chen YN, Yang L, Zhang F, Wang BJ, Zhu YH, Li FY, Yang J, Zhang ZA. A Risk Score Model Incorporating Three m6A RNA Methylation Regulators and a Related Network of miRNAs-m6A Regulators-m6A Target Genes to Predict the Prognosis of Patients With Ovarian Cancer. Front Cell Dev Biol 2021; 9: 703969.
46. Yue Y, Liu J, Cui X, Cao J, Luo G, Zhang Z, Cheng T, Gao M, Shu X, Ma H, Wang F, Wang X, Shen B, Wang Y, Feng X, He C, Liu J. VIRMA mediates preferential m6A mRNA methylation in 3'UTR and near stop codon and associates with alternative polyadenylation. Cell Discov 2018; 4: 10.
47. Barros-Silva D, Lobo J, Guimarães-Teixeira C, Carneiro I, Oliveira J, Martens-Uzunova ES, Henrique R, Jerónimo C. VIRMA-Dependent N6-Methyladenosine Modifications Regulate the Expression of Long Non-Coding RNAs CCAT1 and CCAT2 in Prostate Cancer. Cancers (Basel) 2020; 12: 771.
48. Kurowski MA, Bhagwat AS, Papaj G, Bujnicki JM. Phylogenomic identification of five new human homologs of the DNA repair enzyme AlkB. BMC Genomics 2003; 4: 48.
49. Xu D, Shao W, Jiang Y, Wang X, Liu Y, Liu X. FTO expression is associated with the occurrence of gastric cancer and prognosis. Oncol Rep 2017; 38: 2285-2292.
50. Wen L, Pan X, Yu Y, Yang B. Down-regulation of FTO promotes proliferation and migration, and protects bladder cancer cells from cisplatin-induced cytotoxicity. BMC Urol 2020; 20: 39.
51. Lapeyre-Prost A, Terme M, Pernot S, Marcheteau E, Pointet AL, Voron T, Tartour E, Taïeb J. Immune therapy in colorectal cancer. Colorectal Cancer 2017; 6: 1-10.
52. Cui F, Qu D, Sun R, Nan K. Circulating CD16+CD56+ nature killer cells indicate the prognosis of colorectal cancer after initial chemotherapy. Med Oncol 2019; 36: 84.
53. Chung AS, Wu X, Zhuang G, Ngu H, Kasman I, Zhang J, Vernes JM, Jiang Z, Meng YG, Peale FV, Ouyang W, Ferrara N. An interleukin-17-mediated paracrine network promotes tumor resistance to anti-angiogenic therapy. Nat Med 2013; 19: 1114-1123.
54. Chow C, Wong N, Pagano M, Lun SW, Nakayama KI, Nakayama K, Lo KW. Regulation of APC/CCdc20 activity by RASSF1A-APC/CCdc20 circuitry. Oncogene 2012; 31: 1975-1987.
55. Fischer JM, Miller AJ, Shibata D, Liskay RM. Different phenotypic consequences of simultaneous versus stepwise Apc loss. Oncogene 2012; 31: 2028-2038.
56. Zhu H, Jia X, Wang Y, Song Z, Wang N, Yang Y, Shi X. M6A Classification Combined With Tumor Microenvironment Immune Characteristics Analysis of Bladder Cancer. Front Oncol 2021; 11: 714267.
57. Huang X, Qiu Z, Li L, Chen B, Huang P. m6A regulator-mediated methylation modification patterns and tumor microenvironment infiltration characterization in hepatocellular carcinoma. Aging (Albany NY) 2021; 13: 20698-20715.
58. Qin Q, Fang DL, Zhou W, Meng Y, Wei J. Classification and immune invasion analysis of breast cancer based on m6A genes. Ann Transl Med 2021; 9: 1418.